International Journal of Innovative
Computing, Information and Control
Volume **12**, Number **6**, December **2016**

ICIC International ©2016 ISSN 1349-4198
pp. 1961–1976

IMPROVED BIOGEOGRAPHY-BASED OPTIMIZATION ALGORITHM BASED ON HYBRID HIGH-ORDER MOBILITY MODEL

Jiesheng Wang[1,2] and Jiangdi Song[1]

[1]National Financial Security and System Equipment Engineering Research Center
[2]School of Electronic and Information Engineering
University of Science and Technology Liaoning
No. 185, Qianshan Road, Anshan 114051, P. R. China
wang_jiesheng@126.com; sjd2011@163.com

Received March 2016; revised July 2016

Abstract. *Biogeography-based optimization algorithm (BBO) realizes the information circulation and sharing by using the species migration among habitats and achieves the global optimization by improving habitat adaptability. Based on the information sharing strategy and the population adaptive migration mechanism of BBO algorithm, six new high-order nonlinear hybrid mobility models are proposed based on the cosine-four order mobility model and cosine-sixteen order mobility model. Simulation experiments are carried out to compare the optimization performances of the proposed hybrid high-order mobility models on the typical function optimization problems. The simulation results and analysis show that the proposed improved BBO algorithm has good optimization performance.*

Keywords: Biogeography-based optimization algorithm, Mobility model, Function optimization

1. **Introduction.** The function optimization problem is to find the optimum according to an objective function through some searching strategies [1,2]. The swarm intelligent optimization algorithms, such as ant colony optimization (ACO) algorithm [3], genetic algorithm (GA) [4], particle swarm optimization (PSO) algorithm [5], and artificial bee colony (ABC) algorithm [6], have been applied in the function optimization field successfully. BBO algorithm is a new type of swarm intelligent optimization algorithms and formally put forward by an American scholar Simon in 2008 [7,8], whose basic idea is based on the species migration to complete the information flow between habitats. It achieves information sharing, the suitability improvement of habitats and obtains the optimal solution through adjusting immigration rate and emigration rate, migration topology, migration interval and migration strategies in the process of migration [9].

Compared with other swarm intelligent optimization algorithms, the main advantages of BBO algorithm are little adjusted parameters, simple implementation, fast convergence velocity and high searching precision, which has been successfully applied in economic load assignment [10], combinatorial optimization [11], power distribution of wireless sensor network [12] and function optimization [13], multi-objective path finding in stochastic networks [14], dynamic economic dispatch [15], quadratic assignment problem [16], location area planning [17] and other global optimization problems.

According to the biogeography species distribution, the different linear and nonlinear migration ratio models of biogeography are proposed. Four migration ratio models (exponential migration, quadratic migration, linear migration and cosine migration) are proposed in [18]. Two high-order hybrid migration models (cosine-four order mobility model and cosine-sixteen order mobility model) are proposed in [19]. In order to carry

out further performance validation on the mobility models close to the nature used in the function optimization problems, the emigration rate and immigration rate are set as sine, cosine, linear 4 order and 16 order to produce eight hybrid models to better realize the information sharing of BBO algorithm. Simulation results show that different migration strategies have different influences on the optimization performance of BBO algorithm.

Based on the population adaptive migration mechanism of BBO algorithm, six kinds of high-order nonlinear hybrid mobility model are put forward. Simulation results show that the proposed algorithm has characteristics of high efficiency. The paper is organized as follows. In Section 2, the BBO algorithm is introduced. The hybrid high-order mobility model is presented in Section 3. The simulation experiments and results analysis are introduced in detail in Section 4. Finally, the conclusion is illustrated in the last part.

2. **Biogeography-Based Optimization Algorithm.** The BBO algorithm is derived from the biogeography discipline, which is primarily based on the distribution of species in nature. A diagram illustrating multiple habitats in biological geography is shown in Figure 1.

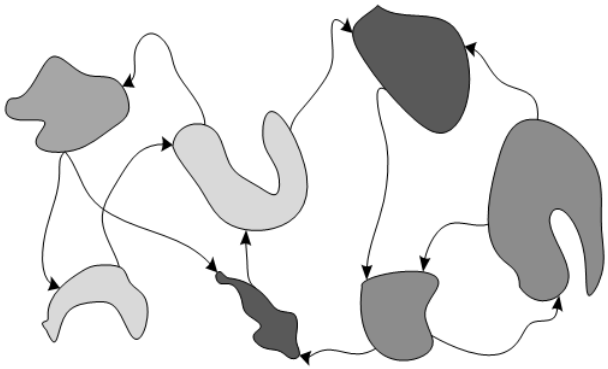

FIGURE 1. Diagram of multi habitats in biological geography

In addition to the relationship among the islands, each island has its own given factors and survival indicators, which is defined as the habitat suitability index (HSI). A probability-based migration operator (habitat migration operator) is set up to enable information sharing among the individuals in the population. The individuals also have their antagonistic emigration rate μ and the immigration rate λ so as to control the movement probability of individuals. A model representing the migration of a single species from an island is shown in Figure 2. Assuming the ratio of emigration and immigration of the species migration model of a single HS is μ and λ, respectively, then the number function of species in the island is established.

It can be seen from Figure 2 that when the number of species is zero, the emigration rate is zero, and when the number of species reaches the maximum capacity of species $S_{\max}$, the emigration rate reaches the maximum value E. Equilibrium is reached at point S_0 when the emigration rate μ is equal to the immigration rate λ. Assuming $E = I$, the situation depicted in Figure 2 can be simplified by reducing it to that shown in Figure 3 and Equations (1) and (2).

$$\mu_k = \frac{E_k}{n} \tag{1}$$

$$\lambda_k = I\left(1 - \frac{k}{n}\right) \tag{2}$$

where $n = S_{\max}$ and k is the number of species.

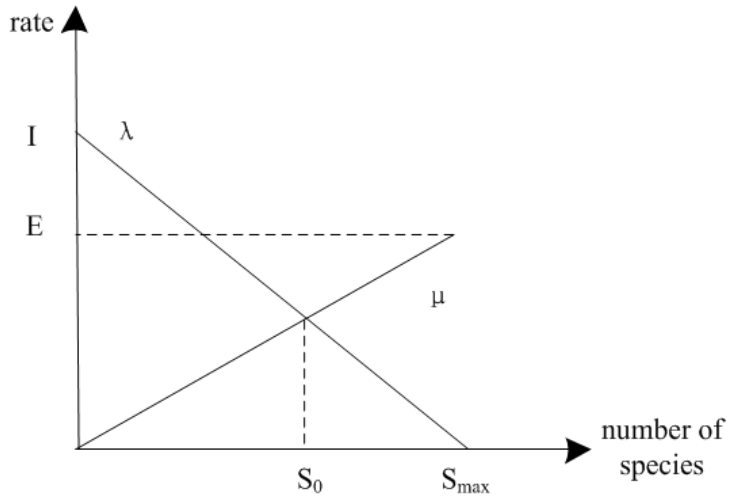

FIGURE 2. Species migration model of single island

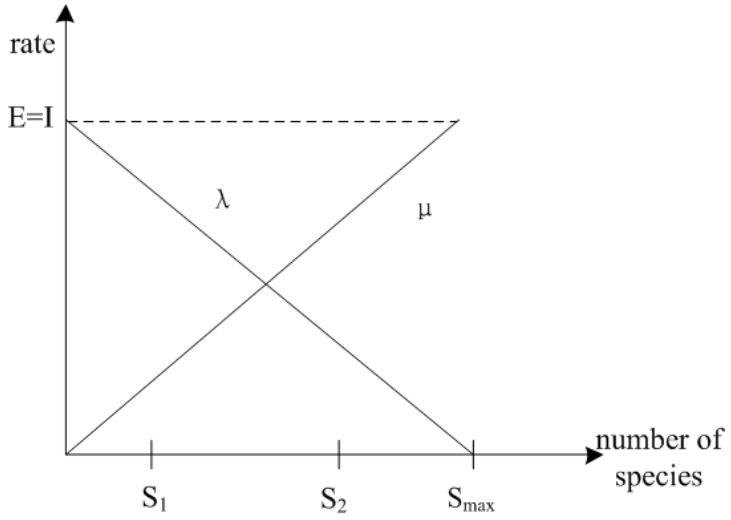

FIGURE 3. Simplified species migration model on single island

The BBO algorithm is a method composed by using n habitats with a D-dimension SIV fitness vector. H_i represents the fitness value of the habitat i. By comparing the habitat values of H_i with $S_{\max}$, the number of all species is denoted as n. Then, the remaining population of the habitat S_i is realized by the successive reduction i according to H_i from good to bad, that is to say $S_i = S_{\max} - i$ $(i = 1, 2, \cdots, n)$. By the above calculation, the emigration rate μ and immigration rate λ of H_i can be obtained for the simplified migration model and the probability $P(K_i)$ of species contained in H_i can be calculated by:

$$M_S = M_{\max} \cdot \left(1 - \frac{P_S}{P_{\max}}\right) \tag{3}$$

Thus, the mutation rate M_i of each H_i is obtained. The global variables are composed of the highest emigration rate E, the immigration rate I, the mutation rate $M_{\max}$, the number of the elite individuals Z and the global migration rate P_{mod} .

3. Hybrid High-Order Mobility Model.

3.1. **Migration ratio model.** According to the biogeography species distribution, different linear and nonlinear migration ratio models of biogeography are obtained, in which four migration ratio models come from [9]; at the same time, other three migration ratio models (sine migration ratio model, migration ratio model with constant emigration rate and migration ratio model with constant immigration rate) are newly put forward shown in Figure 4.

The immigration rate λ_k and the emigration rate μ_k are the function of species diversity k in the habitat; I indicates the maximum immigration rate; E indicates the maximum emigration rate; k_0 is the number of species at the point of habitat equilibrium, that is to say the immigration rate is equal to the emigration rate at that point.

3.1.1. *Exponential migration model.* As shown in Figure 4(a), the immigration rate λ_k and the emigration rate μ_k calculated by Equation (4) are the exponential function of

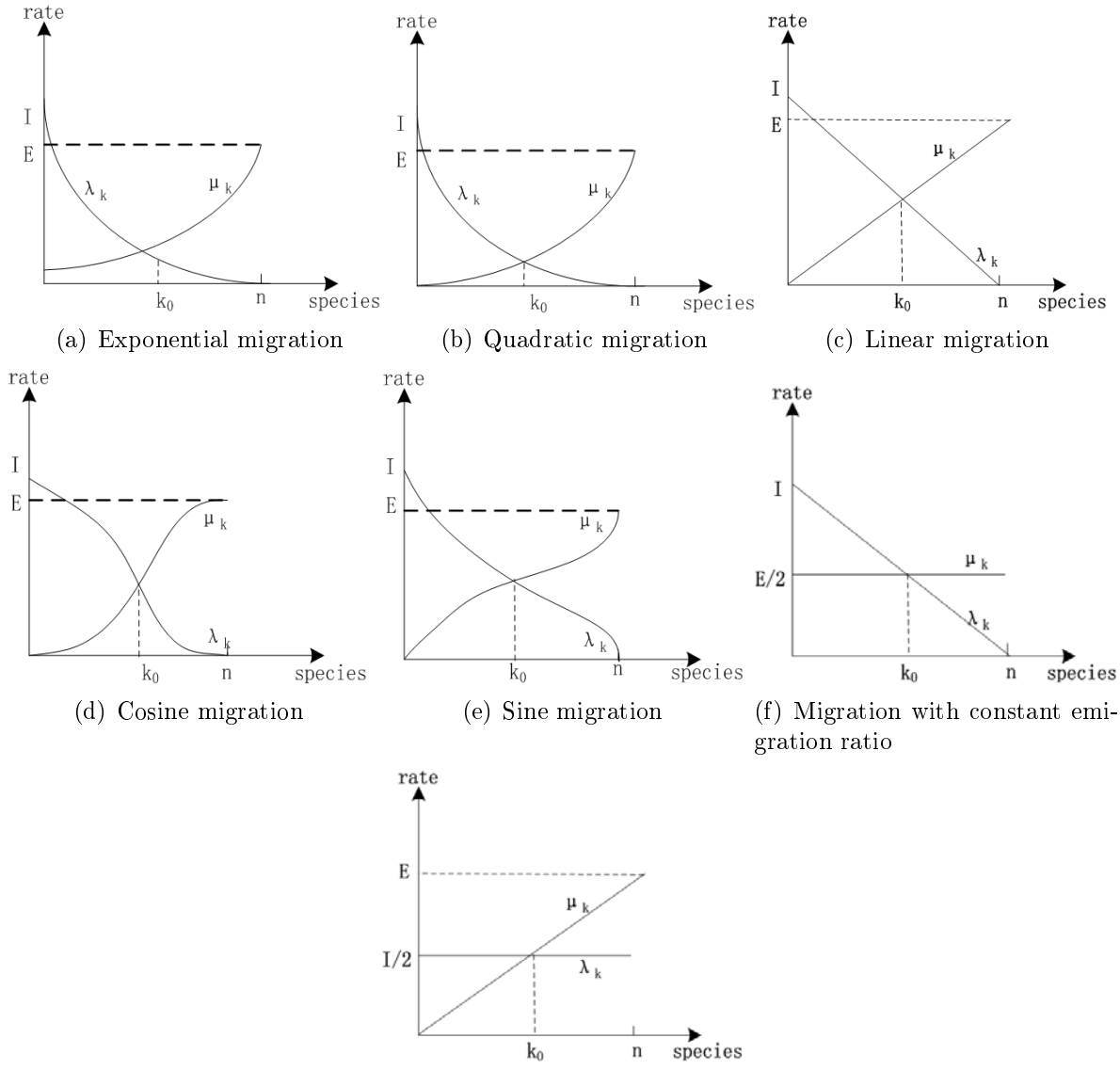

(a) Exponential migration (b) Quadratic migration (c) Linear migration

(d) Cosine migration (e) Sine migration (f) Migration with constant emigration ratio

(g) Migration with constant immigration ratio

FIGURE 4. Seven different migration rate model

species diversity k in the habitat at the exponential migration ratio model (expressed as eBBO).

$$\begin{cases} \lambda_k = Ie^{-\frac{k}{n}} \\ \mu_k = Ee^{\frac{k}{n}-1} \end{cases} \tag{4}$$

3.1.2. *Quadratic migration model.* As shown in Figure 4(b), the immigration rate λ_k and the emigration rate μ_k calculated by Equation (5) are the quadratic function of species diversity k in the habitat at the quadratic migration ratio model (expressed as QBBO).

$$\begin{cases} \lambda_k = I\left(\dfrac{k}{n} - 1\right)^2 \\ \mu_k = E\left(\dfrac{k}{n}\right)^2 \end{cases} \tag{5}$$

3.1.3. *Linear migration model.* As shown in Figure 4(c), the immigration rate λ_k and the emigration rate μ_k calculated by Equation (6) are the linear function of species diversity k in the habitat at the linear migration ratio model (expressed as LBBO).

$$\begin{cases} \lambda_k = I\left(1 - \dfrac{k}{n}\right) \\ \mu_k = E\dfrac{k}{n} \end{cases} \tag{6}$$

3.1.4. *Cosine migration model.* As shown in Figure 4(d), the immigration rate λ_k and the emigration rate μ_k calculated by Equation (7) are the cosine function of species diversity k in the habitat at the cosine migration ratio model (expressed as cBBO).

$$\begin{cases} \lambda_k = \dfrac{I}{2}\left(1 + \cos\left(\dfrac{k\pi}{n}\right)\right) \\ \mu_k = \dfrac{E}{2}\left(1 - \cos\left(\dfrac{k\pi}{n}\right)\right) \end{cases} \tag{7}$$

3.1.5. *Sine migration model.* As shown in Figure 4(e), the immigration rate λ_k and the emigration rate μ_k calculated by Equation (8) are the sine function of species diversity k in the habitat at the sine migration ratio model (expressed as sBBO).

$$\begin{cases} \lambda_k = \dfrac{I}{2}\left(1 + \sin\left(\dfrac{k\pi}{n}\right)\right) \\ \mu_k = \dfrac{E}{2}\left(1 - \sin\left(\dfrac{k\pi}{n}\right)\right) \end{cases} \tag{8}$$

Seen from Figure 4(e), the characteristics of this migration ratio model is contrary to the cosine migration ratio model. When there are fewer or more species in the habitat, the changes of immigration and emigration rates are relatively fast; while the habitat has a number of species, the changes of immigration rate and emigration rate are relatively stable.

3.1.6. *Migration model with constant emigration ratio.* As shown in Figure 4(f), the immigration rate λ_k is the linear function of species diversity k in the habitat and the emigration rate μ_k remains the constant at the migration ratio model with constant emigration ratio (expressed as EBBO), which are calculated by Equation (9).

$$\begin{cases} \lambda_k = I\left(1 - \dfrac{k}{n}\right) \\ \mu_k = \dfrac{E}{2} \end{cases} \tag{9}$$

Seen from Figure 4(f), when there are no species in the inhabit, it has the largest immigration rate I and emigration rate is E/2. With the increase of species diversity, the habitat increasingly becomes crowded, the possibility of immigration becomes smaller, more and more species move to the adjacent inhabits and the emigration rate keeps constant. Finally, when species reach saturation state n, the immigration rate is zero.

3.1.7. *Migration model with constant immigration ratio.* As shown in Figure 4(g), the immigration rate λ_k remains the constant and the emigration rate μ_k is the linear function of species diversity k in the habitat at the migration ratio model with constant immigration ratio (expressed as IBBO), which are calculated by Equation (10).

$$\begin{cases} \lambda_k = \dfrac{I}{2} \\ \mu_k = E\dfrac{k}{n} \end{cases} \tag{10}$$

Seen from Figure 4(g), when there are no species in the inhabit, the immigration rate is $I/2$ and the emigration rate is 0. With the increase of species diversity, the habitat increasingly becomes crowded, and the possibility of immigration remains constant. So the emigration possibility becomes much bigger, namely, more and more species leave to the adjacent habitats. Finally, when species reach saturation state n, the emigration rate is the maximum value E.

3.2. **Hybrid high-order mobility model.** In order to carry out further performance validation on the mobility models close to the nature used in the function optimization problems, based on the cosine, sine and secondary model, the arbitrary two methods are combined to produce the hybrid models. In order to deepen the contrast effect, the emigration rate and immigration rate are set as sine, cosine, linear 4 order and 16 order to realize the hybrid models, respectively. Thus, a total of eight kinds of high-order hybrid migration models are produced.

Based on the cosine-four order mobility model (M4-1) and cosine-sixteen order mobility model (M4-2) proposed in [18], six high-order hybrid migration models are proposed. They are listed as four order-cosine mobility model (M4-3), sixteen order-cosine mobility model (M4-4), sine-four order mobility model (M5-1) and sine-sixteen order mobility model (M5-2), four order-sine mobility model (M5-3) and sixteen order-sine mobility model (M5-4). These eight models are shown in Figures 5(a)-5(h). The expression formulas are listed in Table 1 for the hybrid models.

4. **Simulation Experiments and Results Analysis.** Under the same simulation environment with the software MATLAB and the same parameters initialization for all kinds of BBO algorithm, the proposed improved BBO algorithm with the hybrid high-order migration models carries out simulation experiments on six typical function optimization problems. The experiments for each function are run independently 100 times. Among them, the Rastrigin, Griewank and Ackley functions are complex nonlinear multimodal functions, which are used to measure whether the algorithm can avoid prematurity and the ability to find global optimal solution. The Sphere, Rosenbrock and Step are single mode function, which are used to test the algorithm optimization precision and the

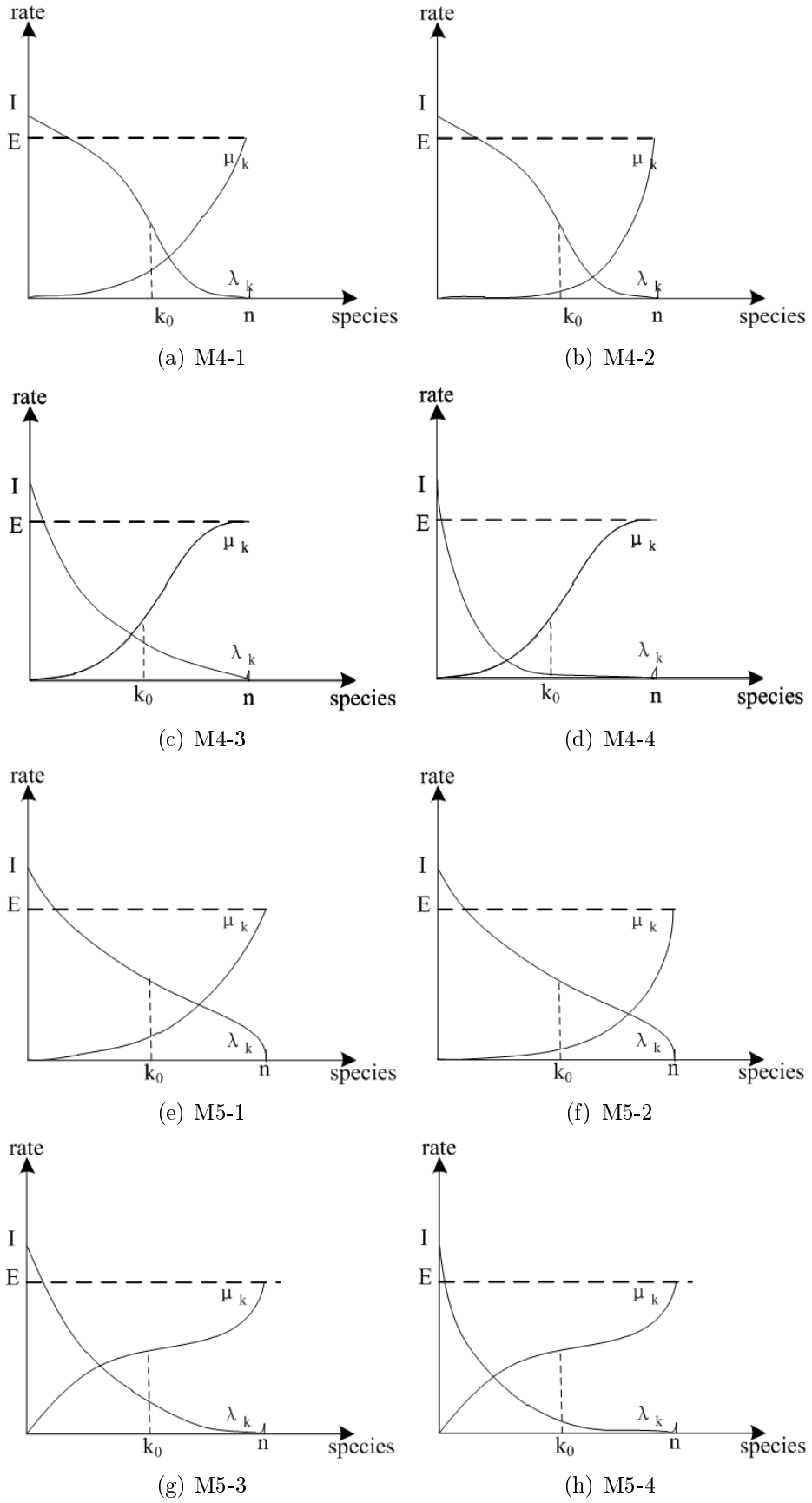

(a) M4-1 (b) M4-2

(c) M4-3 (d) M4-4

(e) M5-1 (f) M5-2

(g) M5-3 (h) M5-4

FIGURE 5. Curves of hybrid models

TABLE 1. Expression of hybrid model

Model	Expression	Model	Expression
M4-1	$\lambda_k = \frac{I}{2}\left(1+\cos\left(\frac{k\pi}{n}\right)\right)$ $\mu_k = E\left(\frac{k}{n}\right)^4$	M5-1	$\lambda_k = \frac{I}{2}\left(1+\sin\left(\frac{k\pi}{n}\right)\right)$ $\mu_k = E\left(\frac{k}{n}\right)^4$
M4-2	$\lambda_k = \frac{I}{2}\left(1+\cos\left(\frac{k\pi}{n}\right)\right)$ $\mu_k = E\left(\frac{k}{n}\right)^{16}$	M5-2	$\lambda_k = \frac{I}{2}\left(1+\sin\left(\frac{k\pi}{n}\right)\right)$ $\mu_k = E\left(\frac{k}{n}\right)^{16}$
M4-3	$\lambda_k = I\left(1-\frac{k}{n}\right)^4$ $\mu_k = \frac{E}{2}\left(1-\cos\left(\frac{k\pi}{n}\right)\right)$	M5-3	$\lambda_k = I\left(1-\frac{k}{n}\right)^4$ $\mu_k = \frac{E}{2}\left(1-\sin\left(\frac{k\pi}{n}\right)\right)$
M4-4	$\lambda_k = I\left(1-\frac{k}{n}\right)^{16}$ $\mu_k = \frac{E}{2}\left(1-\cos\left(\frac{k\pi}{n}\right)\right)$	M5-4	$\lambda_k = I\left(1-\frac{k}{n}\right)^{16}$ $\mu_k = \frac{E}{2}\left(1-\sin\left(\frac{k\pi}{n}\right)\right)$

TABLE 2. Simulation optimal and average solution for function optimization

Model	Rastrigin		Griewank		Ackley		Sphere		Rosenbrock		Step	
	Best	Mean	Best	Mean	Best	Mean	Best	Mean	Best	Mean	Best	Mean
M4	9.84	20.32	1.63	6.86	3.90	7.32	0.23	2.96	22.64	125.31	102	826.18
M4-1	11.60	22.71	1.83	23.83	3.81	5.91	0.19	6.31	22.21	98.40	94	881.8
M4-2	10.94	20.73	2.11	12.45	**3.69**	6.76	0.24	3.26	21.53	99.56	107	1069.36
M4-3	10.85	19.23	1.90	10.63	4.08	6.06	0.21	2.18	24.52	428.92	107	860.38
M4-4	7.99	16.56	**1.45**	4.47	3.70	6.26	0.19	**1.94**	24.63	96.61	**71**	1104.12
M5	9.58	17.39	1.68	6.38	3.80	6.38	0.25	4.08	22.98	168.85	104	1366.88
M5-1	10.94	18.11	1.98	**3.96**	3.80	6.54	0.14	2.75	**18.39**	**71.21**	77	**739.22**
M5-2	10.02	19.80	1.71	7.41	4.04	**5.34**	**0.13**	3.04	19.21	93.65	97	755.7
M5-3	**6.90**	**15.77**	1.70	8.86	3.80	6.31	0.20	2.34	21.07	197.91	76	1141.64
M5-4	8.08	21.14	1.52	14.86	3.95	6.48	0.24	2.18	23.19	201.56	82	1758.16

convergence property of the proposed algorithms. The optimization curves are shown in Figures 6-11. The optimal solution and the average solution obtained from function simulation experiments are listed in Table 2.

All M4 series simulation results are shown in Figures 6(a)-11(a) and M5 in Figures 6(b)-11(b). It can be seen from the simulation curves that besides Ackley function, the overall convergence velocity rates of Figures 6(a)-11(a) for other five functions were significantly higher than Figures 6(b)-11(b). The convergence speed of function Step is the fastest and it tends to be stable after 20 simulation iterations. The functions Griewank and Sphere tend to a stable state after 50 iterations. The function Rastrigin after 50 times tends to a stable state, and iterative Rastrigin function is stable after 80. In Figures 6(a)-11(a), M4-4 has the best optimization performance and M4 is the worst. In Figures 6(b)-11(b), the optimization effect of M5-3 is the best and M5-4 is the worst. In conclusion,

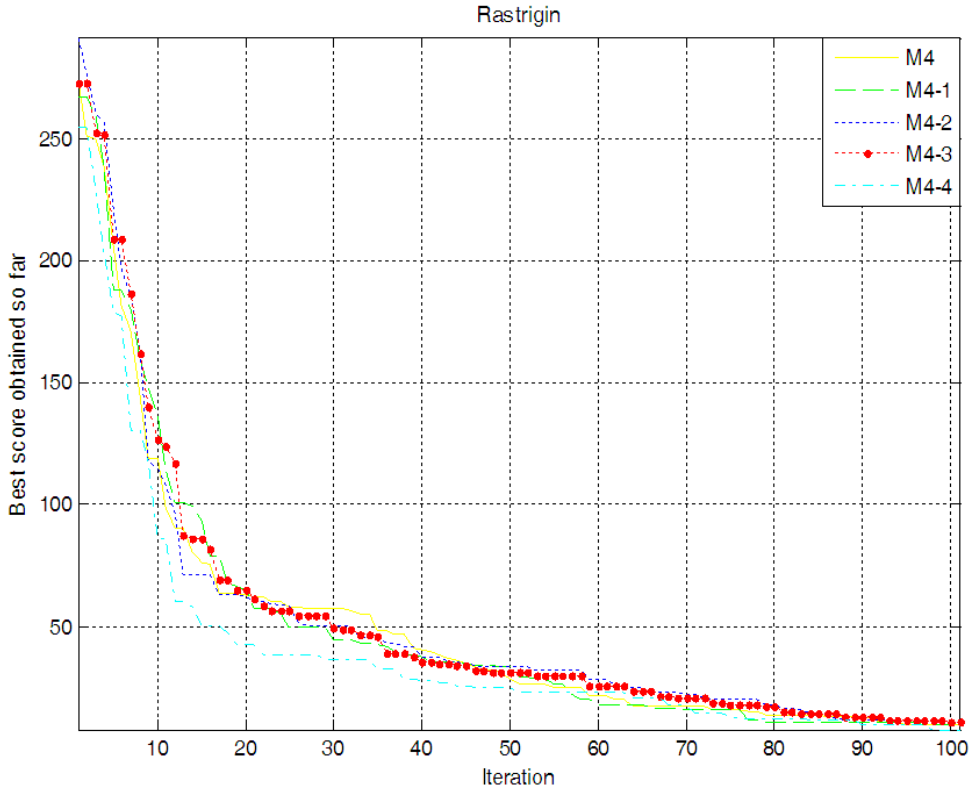

(a) Rastrigin

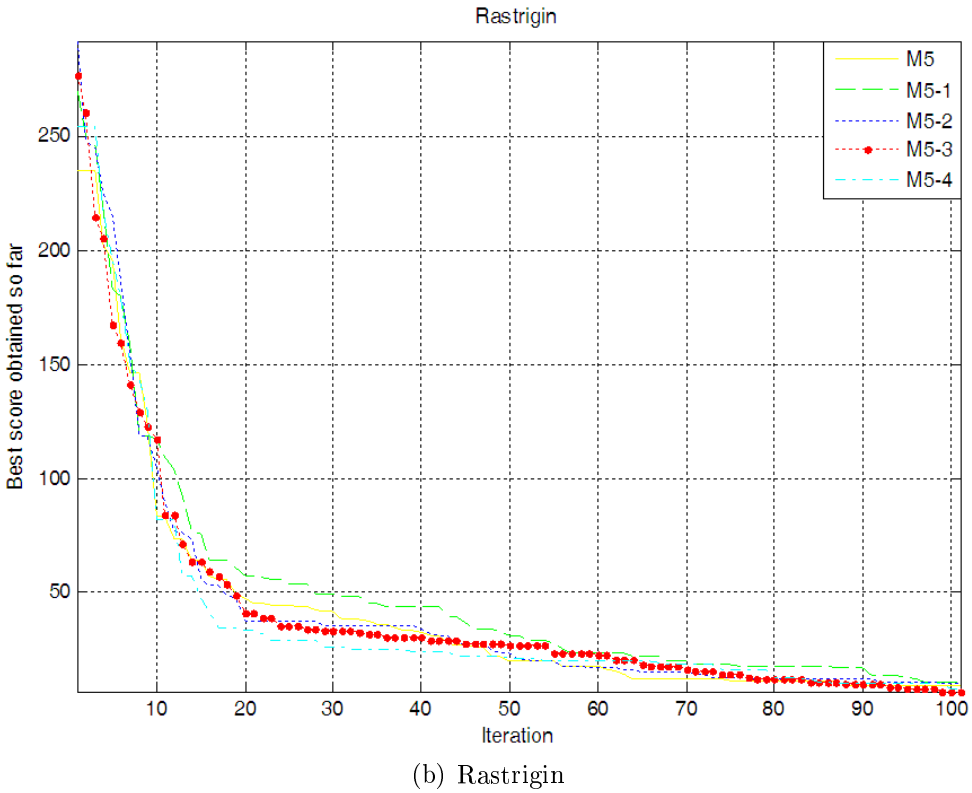

(b) Rastrigin

FIGURE 6. Simulation curves on hybrid high times models of BBO

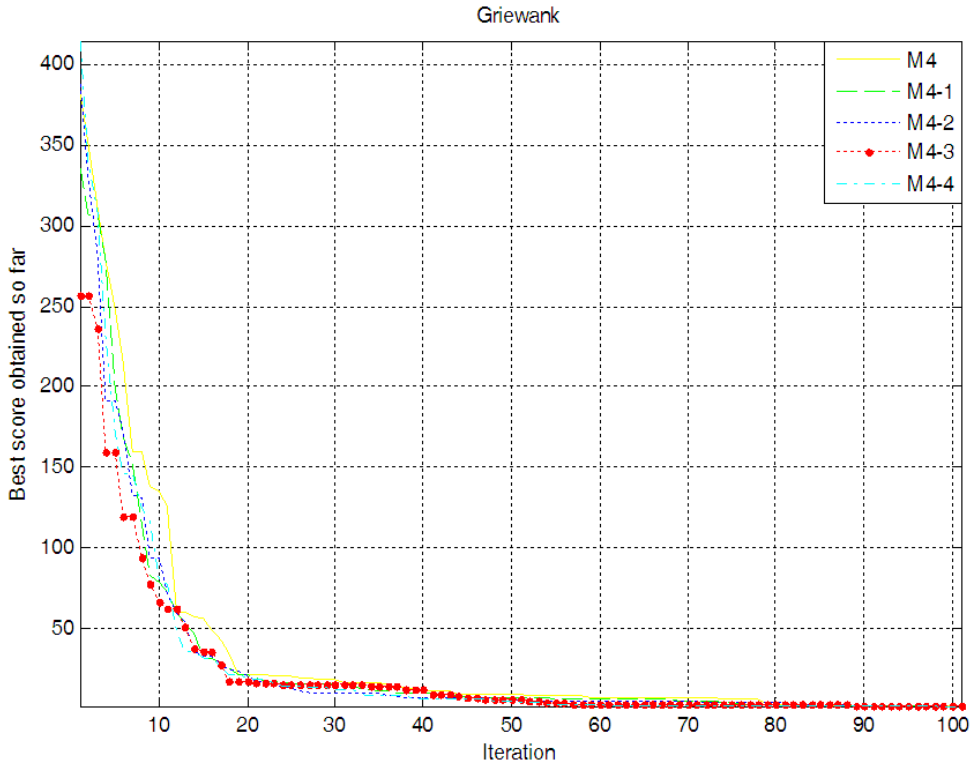

(a) Griewank

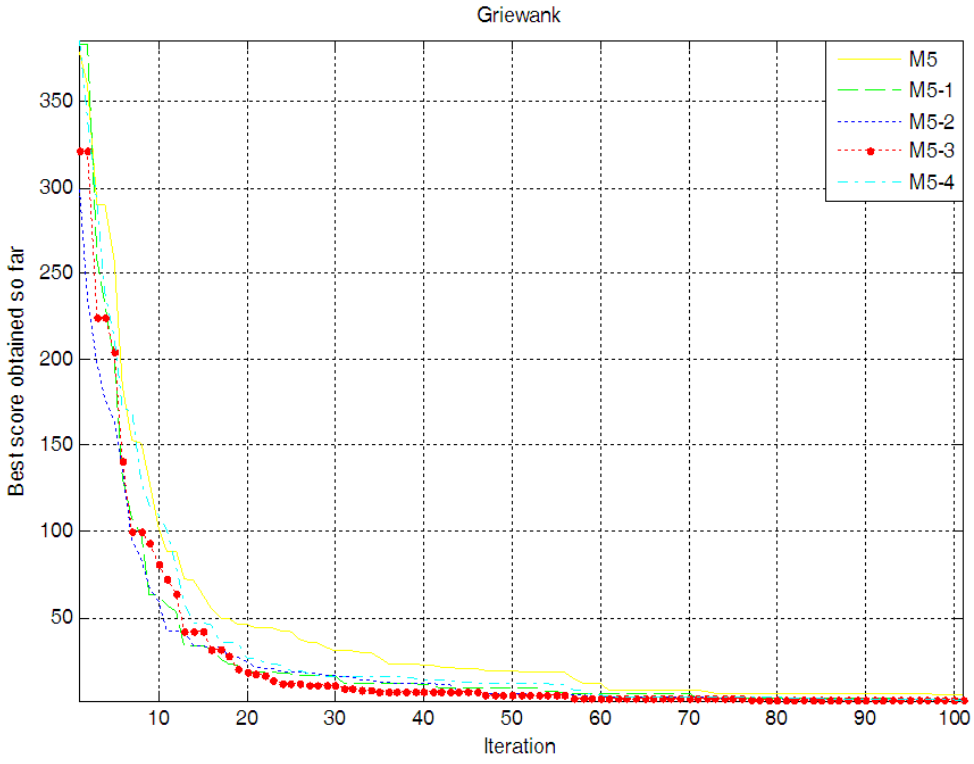

(b) Griewank

FIGURE 7. Simulation curves on hybrid high times models of BBO

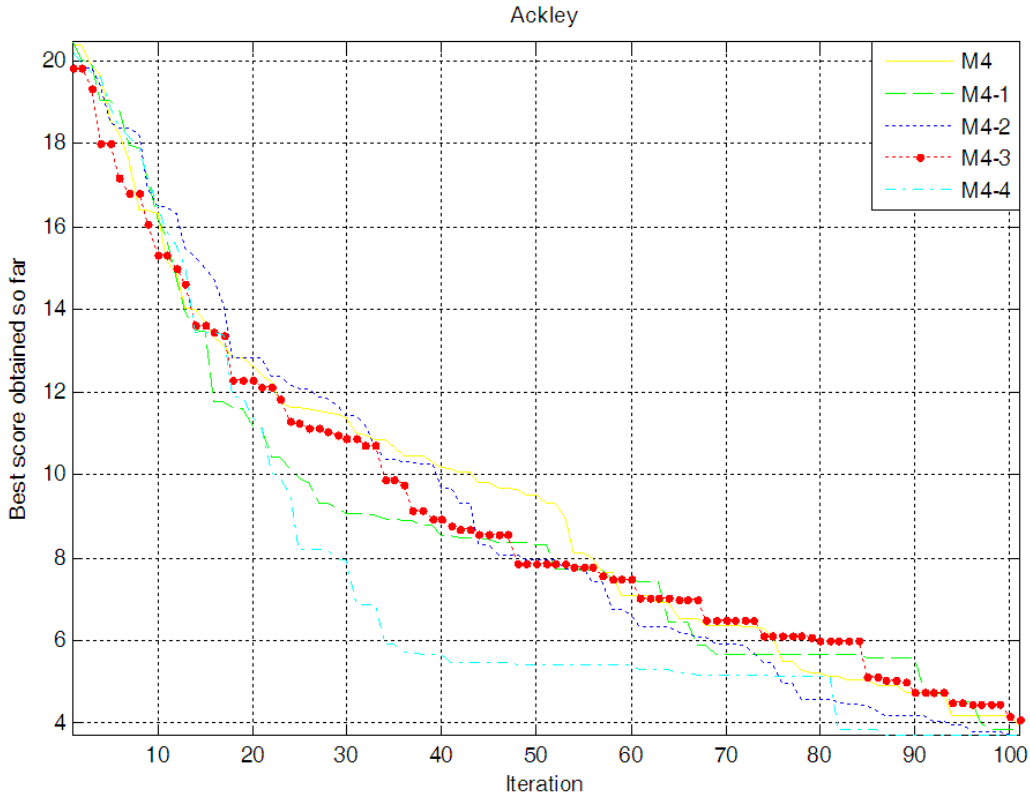

(a) Ackley

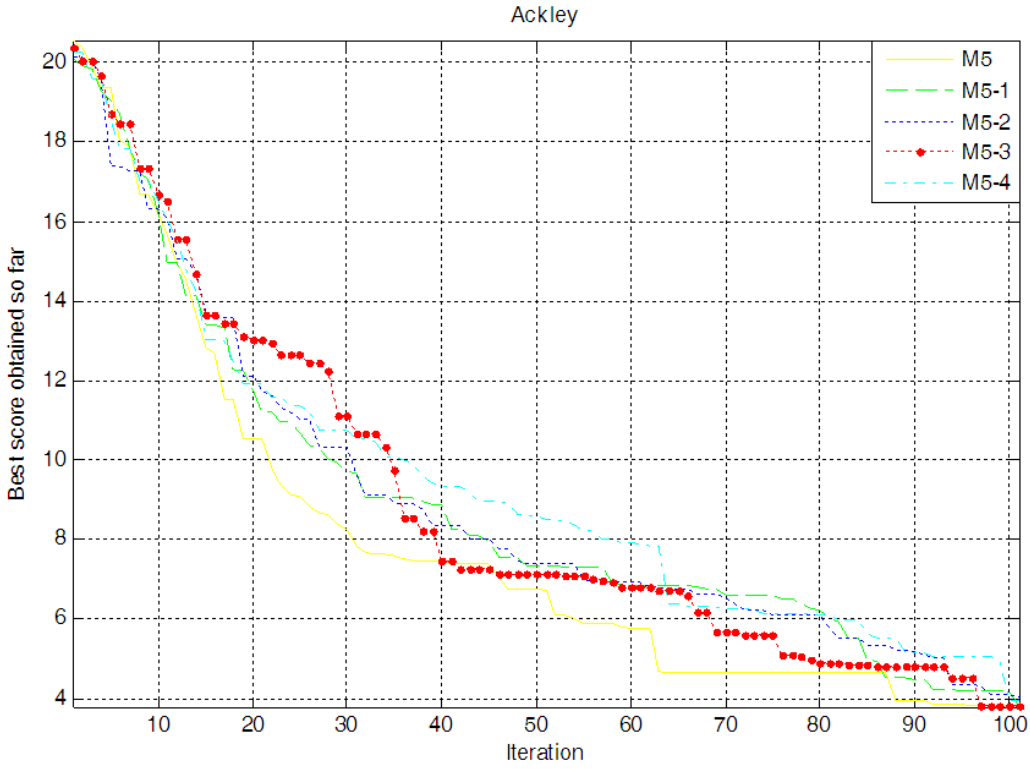

(b) Ackley

FIGURE 8. Simulation curves on hybrid high times models of BBO

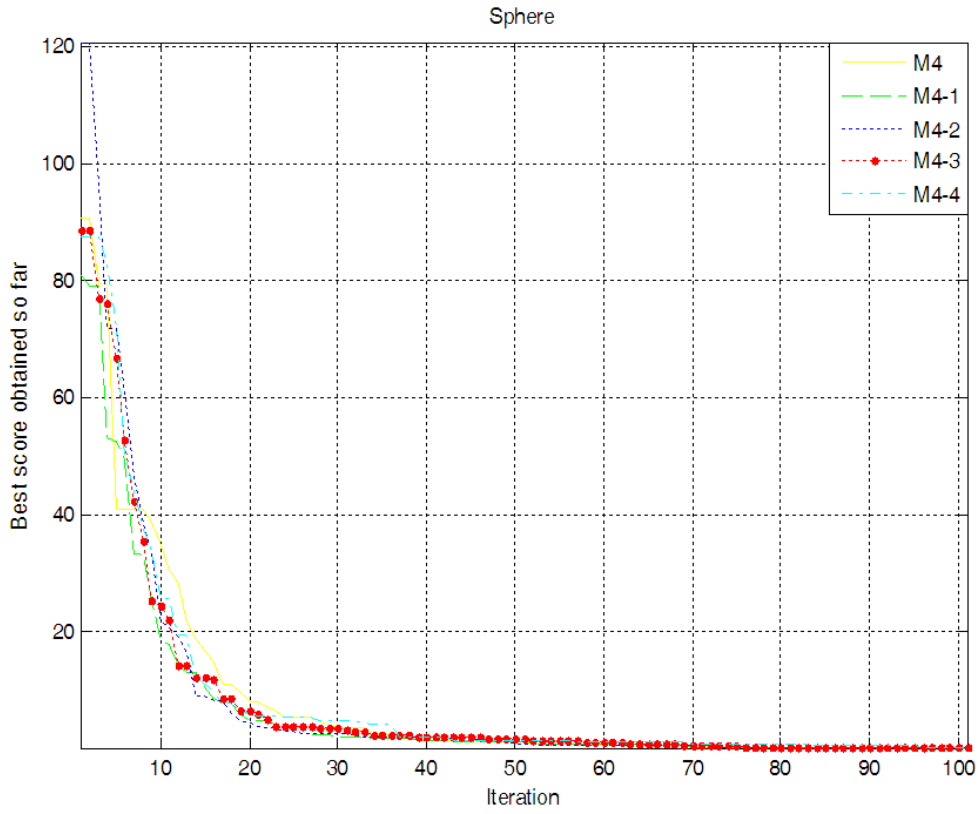

(a) Sphere

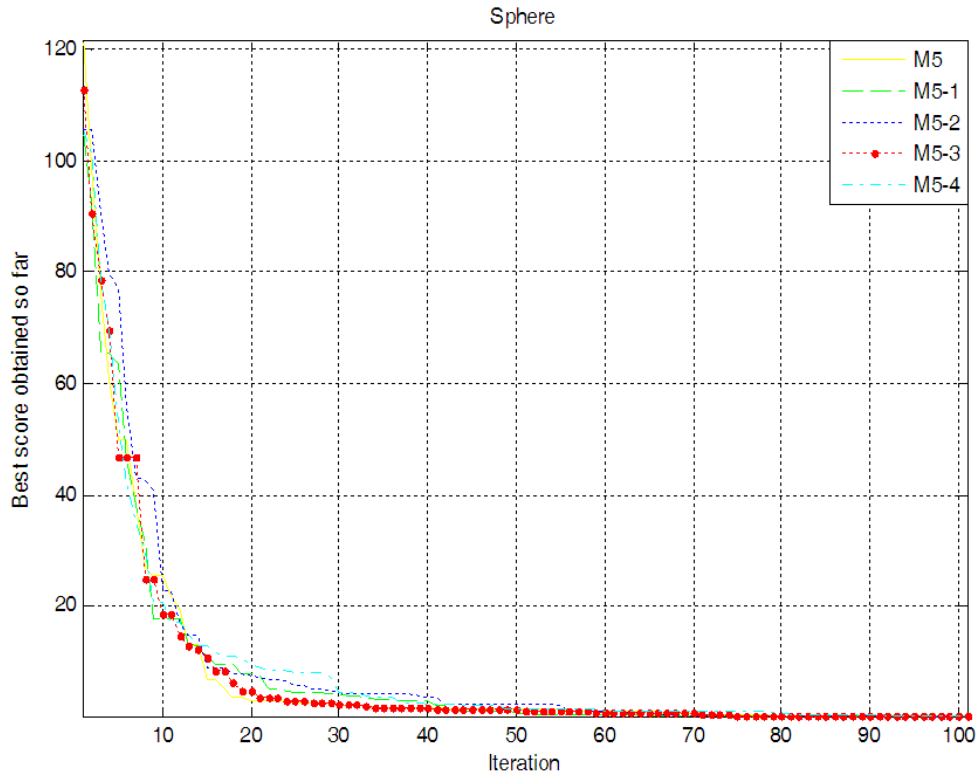

(b) Sphere

FIGURE 9. Simulation curves on hybrid high times models of BBO

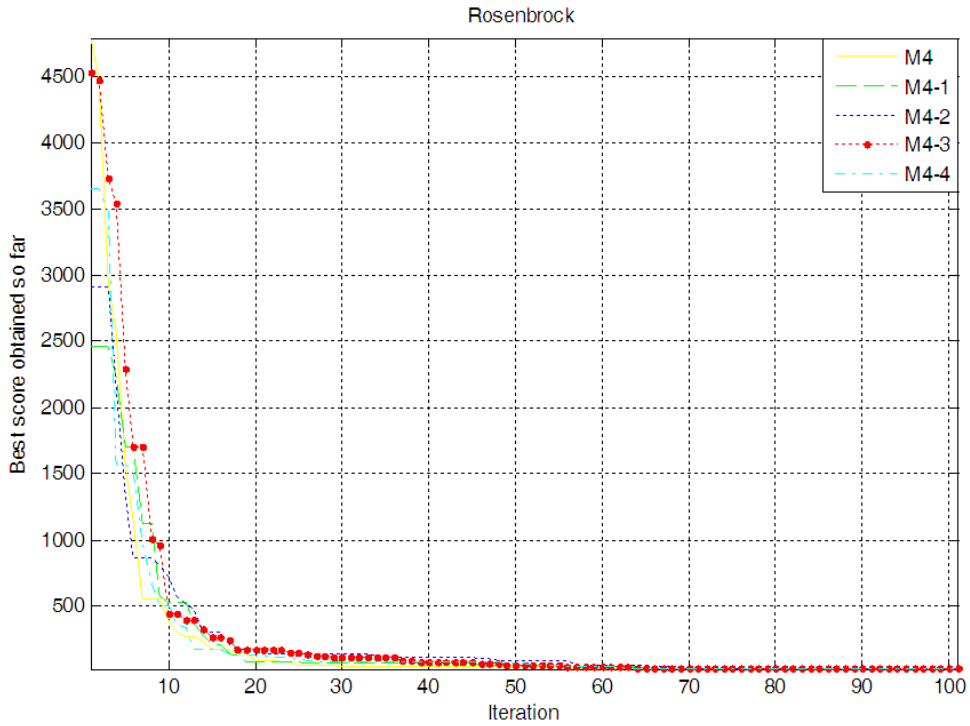

(a) Rosenbrock

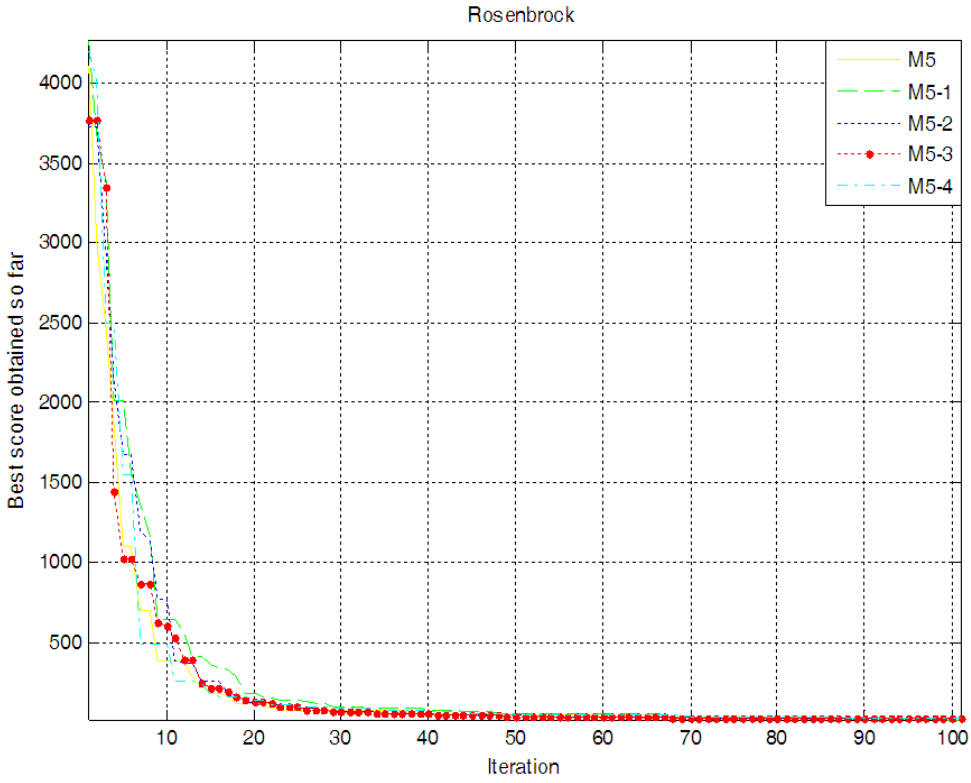

(b) Rosenbrock

FIGURE 10. Simulation curves on hybrid high times models of BBO

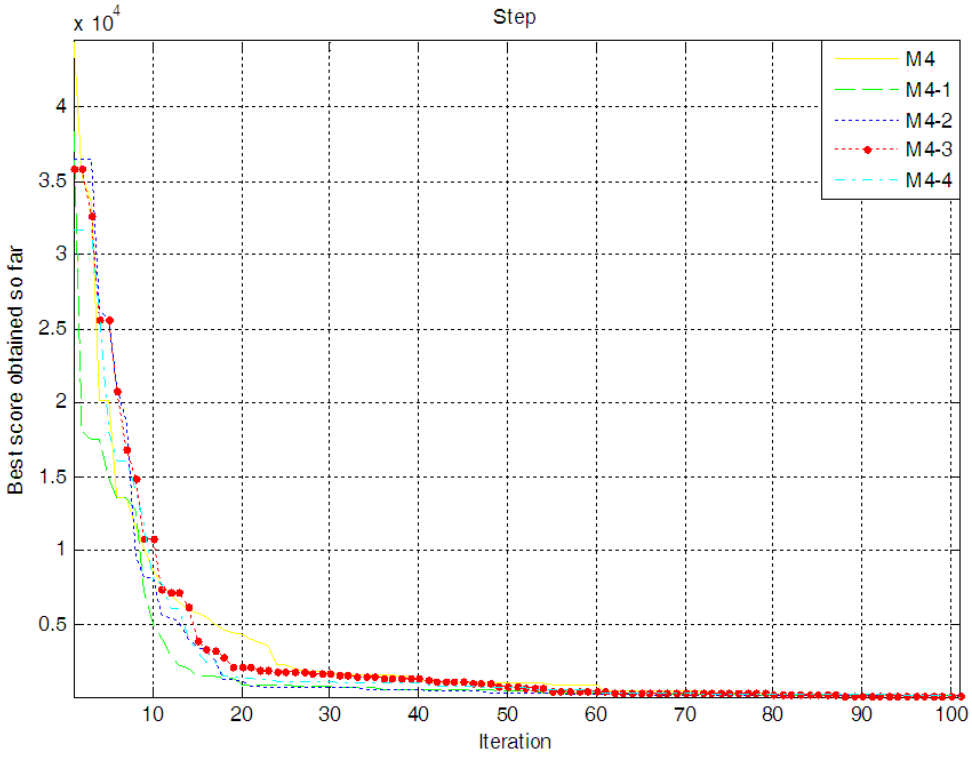

(a) Step

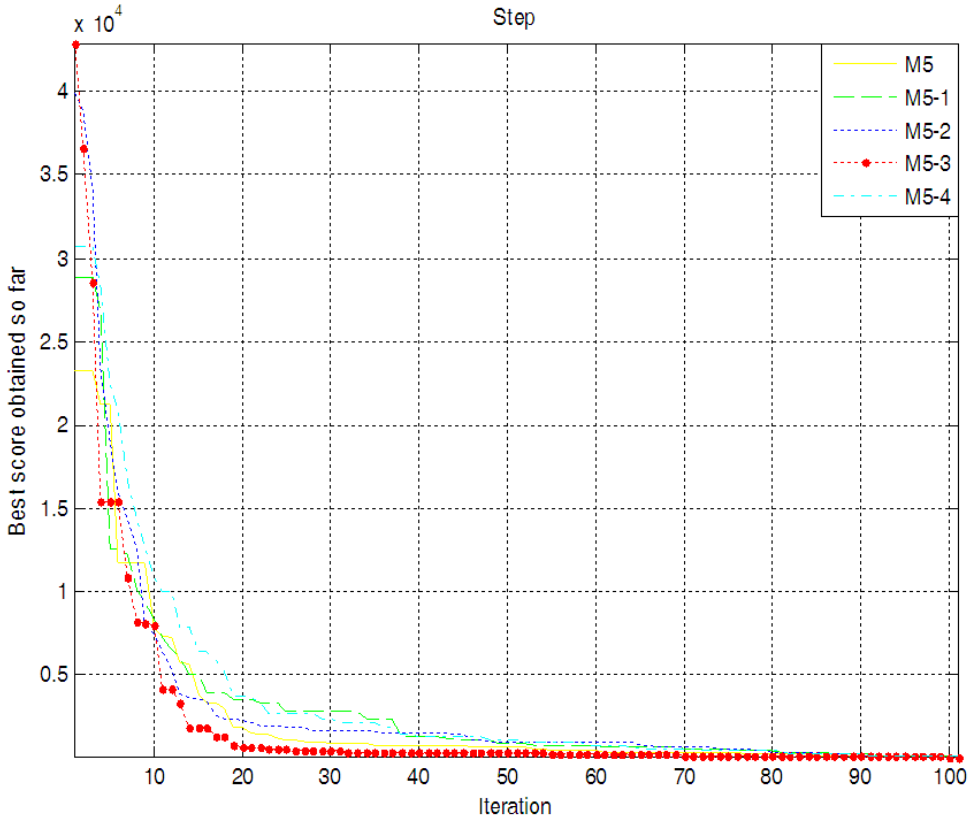

(b) Step

FIGURE 11. Simulation curves on hybrid high times models of BBO

simulation results and analysis show that the sine functions (M5-1 and M5-2) have better optimization performance than other high-order nonlinear hybrid mobilities. On the other hand, it can be seen from Table 2 that the optimal and average solution by adopting sine function as the immigration rate or emigration rate are better than cosine function. Also M5 and M5-3 all obtain the optimum for Rastrigin function and Rosenbrock function. This shows the superiority of sine function. In addition, the emigration rate of M5-1 is linear four-order and the immigration rate of M4-4 is linear sixteen-order. These two models obtain the optimal solution at the most times, which shows that the linear higher order migration model has important influence on the performances of solving the function optimization problems.

5. **Conclusions.** In this paper, six new high-order nonlinear hybrid mobility models are proposed based on the cosine-four order mobility model (M4-1) and cosine-sixteen order mobility model (M4-2) proposed in [19]. Simulation results and analysis show that the proposed improved BBO algorithm based on six high-order nonlinear hybrid mobility have good optimization performance than other two high-order nonlinear hybrid mobilities. In future, research on other migration models and hybrid BBO algorithm combining with other swarm intelligent optimization algorithms will be carried out and the research results are applied in the industrial process control fields.

Acknowledgment. This work is partially supported by the Program for Liaoning Excellent Talents in University (Grant No. LR2014008), the Project by Liaoning Provincial Natural Science Foundation of China (Grant No. 2014020177), the Program for Research Special Foundation of University of Science and Technology of Liaoning (Grant No. 2015TD04) and the Opening Project of National Financial Security and System Equipment Engineering Research Center (Grant Nos. USTLKFGJ201502 and USTLKEC 201401).

REFERENCES

[1] Y. Ren and Y. Wu, An efficient algorithm for high-dimensional function optimization, *Soft Computing*, vol.17, no.6, pp.995-1004, 2013.

[2] A. K. Kar, Bio inspired computing – A review of algorithms and scope of applications, *Expert Systems with Applications*, vol.59, pp.20-32, 2016.

[3] H. F. Kuo, Ant colony optimization-based freeform sources for enhancing nanolithographic imaging performance, *IEEE Trans. Nanotechnology*, vol.15, no.4, p.1, 2016.

[4] M. Fogue, J. A. Sanguesa, F. Naranjo, J. Gallardo, P. Garrido and F. J. Martinez, Non-emergency patient transport services planning through genetic algorithms, *Expert Systems with Applications*, vol.61, pp.262-271, 2016.

[5] M. Clerc and J. Kennedy, The particle swarm – Explosion, stability, and convergence in a multidimensional complex space, *IEEE Trans. Evolutionary Computation*, vol.6, no.1, pp.58-73, 2002.

[6] Z. Li, W. Wang, Y. Yan and Z. Li, PS-ABC: A hybrid algorithm based on particle swarm and artificial bee colony for high-dimensional optimization problems, *Expert Systems with Applications*, vol.42, no.22, pp.8881-8895, 2015.

[7] D. Simon, Biogeography-based optimization, *IEEE Trans. Evolutionary Computation*, vol.12, no.6, pp.702-713, 2008.

[8] D. Simon, A probabilistic analysis of a simplified biogeography-based optimization algorithm, *Evolutionary Computation*, vol.19, no.2, pp.167-188, 2011.

[9] H. Ma, An analysis of the equilibrium of migration models for biogeography-based optimization, *Information Sciences*, vol.180, no.18, pp.3444-3464, 2010.

[10] A. Bhattacharya and P. K. Chattopadhyay, Hybrid differential evolution with biogeography-based optimization for solution of economic load dispatch, *IEEE Trans. Power Systems*, vol.25, no.4, pp.1955-1964, 2010.

[11] M. Ergezer and D. Simon, Oppositional biogeography-based optimization for combinatorial problems, *Proc. of the 2011 IEEE Congress on Evolutionary Computation (CEC)*, New Orleans, LA, USA, pp.1496-1503, 2011.

[12] W. Gong, Z. Cai, C. X. Ling and H. Li, A real-coded biogeography-based optimization with mutation, *Applied Mathematics and Computation*, vol.216, no.9, pp.2749-2758, 2010.

[13] I. Boussaid, A. Chatterjee, P. Siarry and M. Ahmed-Nacer, Hybridizing biogeography-based optimization with differential evolution for optimal power allocation in wireless sensor networks, *IEEE Trans. Vehicular Technology*, vol.60, no.5, pp.2347-2353, 2011.

[14] S. Wang, J. Yang, G. Liu, S. Du and J. Yan, Multi-objective path finding in stochastic networks using a biogeography-based optimization method, *Simulation Transactions of the Society for Modeling & Simulation International*, vol.92, no.7, pp.637-647, 2016.

[15] U. Krishnasamy and D. Nanjundappan, Hybrid weighted probabilistic neural network and biogeography based optimization for dynamic economic dispatch of integrated multiple-fuel and wind power plants, *International Journal of Electrical Power & Energy Systems*, vol.77, pp.385-394, 2016.

[16] L. W. Loon, W. Antoni, D. M. Ishak and H. Habibollah, A biogeography-based optimization algorithm hybridized with tabu search for the quadratic assignment problem, *Computational Intelligence & Neuroscience*, vol.2016, no.2, pp.1-12, 2016.

[17] S. S. Kim, J. H. Byeon, S. Lee and H. Liu, A grouping biogeography based optimization for location area planning, *Neural Computing & Applications*, vol.26, no.8, pp.2001-2012, 2015.

[18] W. Guo, L. Wang and Q. Wu, An analysis of the migration rates for biogeography-based optimization, *Information Sciences*, vol.254, no.19, pp.111-140, 2014.